Inferring Cortical Subdivisions Based on Skull Morphology

3

Yasushi Kobayashi, Toshiyasu Matsui, and Naomichi Ogihara

Abstract

Reconstructing brains of fossil hominids is one of the most important issues in anthropology. It is of particular interest to know the extent of cortical subdivisions in those brains since differences may indicate the differences in cognitive capabilities between fossil hominines and modern humans. We evaluated two approaches to infer borders of cortical regions based on skull morphology. The first approach is to identify cerebral sulci and gyri based on the surface morphology of endocasts. The second approach is to infer the location of cerebral sulci and gyri using their spatial relationship with cranial sutures and other landmarks. We review the historical origin of these two approaches and evaluate their validity in fossil hominine studies.

Keywords

Endocast • Suture • Sulcus • Cortical areas • Prefrontal cortex • Primate

3.1 Introduction

Knowing the characteristics of cognitive functions in fossil hominids is one of the most essential targets, not only in studies on those extinct species but also in understanding the nature of modern humans. Cognitive functions are implemented in the nervous system, particularly in the brain. Today, neuroscience has a great variety of research tools that elucidate the structure and function of the nervous system and monitor their changes. Recent techniques using molecular biology and pharmacology can even manipulate specific functions of the nervous system. However, for studies on fossil hominids, we can only use remaining hard tissues and infer the structure and functions of the nervous system from them.

In this chapter, we first review the structures of the brain that may differentiate our cognitive functions from those of fossil hominids and present two approaches to infer the extent of some parts of the brain based on the skull morphology. We primarily focus on the differences between modern humans and Neanderthals but also refer to important studies in other fossil hominids, as well as extant primate species.

3.2 Classical Views in Primate Brain Evolution

The most outstanding feature of the primate brain is the highly developed cerebral cortex. The volume of the brain, and its subregions, has been quantitatively analyzed using allometry. Jerison defined the "encephalization quotient" (EQ) to quantify the relative development of brain volume to body size and clearly showed that extant mammals possess larger brains than fossil mammals and extant reptiles of similar body weight (Jerison 1973).

Y. Kobayashi (✉) • T. Matsui
Department of Anatomy and Neurobiology, National Defense Medical College, Tokorozawa, Saitama, Japan
e-mail: yasushi@ndmc.ac.jp; matsuto@ndmc.ac.jp

N. Ogihara
Department of Mechanical Engineering, Faculty of Science and Technology, Keio University, Yokohama, Kanagawa, Japan
e-mail: ogihara@mech.keio.ac.jp

E. Bruner et al. (eds.), *Digital Endocasts*, Replacement of Neanderthals by Modern Humans Series,
DOI 10.1007/978-4-431-56582-6_3

Although Jerison discussed the importance of EQ as an index of intelligence applicable to a wide variety of species, behavioral and cognitive studies in primates provided somewhat different views concerning brain organization and intelligence. Based on these findings, absolute brain size and body size are considered to better correlate with the mental performance of nonhuman primates than EQ (see review by Gibson et al. 2001).

The proportions of the volume of different subdivisions of the brain are also informative when we evaluate different aspects of neural functions. Stephan focused on the "ascending primate scale"—a series of different classes of species comprising basic insectivores, progressive insectivores, prosimians, and simians—and defined the "encephalization index," the relative brain volume of a primate species compared to a basic insectivore of equal body weight (Stephan and Andy 1969). His data showed that brains of simians are larger than those of prosimians, which are in turn larger than those of insectivores. He also calculated the progression indices, a value expressing the degree of enlargement of a structure in one species in comparison with that of a typical basal insectivore of equal body weight. The simian neocortex exhibited by far the highest progression index, followed by the striatum, the diencephalon, and the cerebellum.

The neocortex is a division of the cerebral cortex, which underwent overwhelmingly rapid development during primate evolution. It was originally defined as the part of the cerebral cortex that does not receive direct or indirect inputs of olfactory information (Ariëns Kappers 1909). It roughly corresponds to the isocortex, which typically shows six-layered organization either in the adult or during development (Brodmann 1906). The isocortex did not expand uniformly throughout primate evolution but subdivided into relatively stable primary sensory- and motor-related areas and rapidly expanding association areas.

The association areas are regions of the cerebral cortex that are myelinated later than primary sensory and motor-related areas during development (Flechsig 1920). The association areas receive sensory information from primary sensory areas, integrate different sensory modalities, identify and locate objects, judge the surrounding environment, store and retrieve long-term memories, and plan and execute behaviors. They, thus, play a pivotal role in higher cognitive functions, especially in primates.

The association areas are roughly subdivided into frontal, parietal, occipital, and temporal. The frontal association areas (prefrontal areas) are bordered caudally by motor-related areas, mostly the premotor area. In the primate, the border on the lateral surface largely corresponds to the precentral sulcus. The parietal association areas are bordered rostrally by the postcentral sulcus, separating them from the primary somatosensory area, and the occipital association areas are separated from the primary visual area (V1) by the lunate sulcus running caudally. However, borders between the parietal, occipital, and temporal association areas are not macroscopically obvious, except for the parieto-occipital sulcus on the medial surface and the preoccipital notch on the latero-inferior margin. Accordingly, these association areas are often referred to together as the parieto-temporo-occipital association areas.

To demonstrate the evolutional changes of the primate association areas, Brodmann (1912) measured the surface area of the frontal association areas "regio frontalis," motor-related areas "regio precentralis," and total frontal lobe "Frontallappen" (Table 3.1). The data clearly showed that frontal association areas (prefrontal areas) expanded during primate evolution, particularly in greater apes and the modern human. The proportion of the motor-related areas remained rather stable from old-world monkey to greater apes, but markedly reduced in the modern human, probably due to the expansion of association areas, not only in the frontal association areas but also in the parieto-temporo-occipital association areas.

Blinkov and Glezer (1968) also measured the surface area of the cerebral cortex and showed that the proportion of the human frontal cortex in the whole brain was by far the largest in primate species (32.8% in human, 22.1% in chimpanzee, 21.3% in orangutan, 21.2% in gibbons).

The cerebral cortex did not expand alone during evolution. In addition to association and commissural connections between different cortical areas, the cortex has robust projections to and from different subcortical structures, which also developed, keeping step with cortical changes during evolution. The portion of the white matter that interconnects these structures expanded as well.

Table 3.1 Proportion of the surface area of the prefrontal and frontal cortices to that of the total cerebral cortex according to Brodmann (1912)

Species	Regions		
	"Regio frontalis" (prefrontal areas)	"Regio precentralis" (areas 4 and 6)	"Frontallappen" (frontal lobe)
Rabbit	2.2%		
Cat	3.4%		
Dog	6.9%		
Lemur	7.2–8.3%		
Marmoset	8.9%		
Capuchin	9.2%	13.3%	22.5%
Guenon	11.1%	13.5%	24.6%
Macaque	11.3%	11.9%	23.2%
Hylobates	11.3%	10.1%	21.4%
Chimpanzee	16.9%	13.6%	30.5%
Human	29.0%	7.3%	36.3%

3.3 Updated Information on Primate Brain Evolution

Advances in modern neuroanatomical and imaging studies also provided abundant quantitative data on the organization of the brain in extant primate species, including humans. Recent studies by Herculano-Houzel provided a totally new approach to estimate the magnitude of development of the mammalian brains including primates. They homogenized tissue and counted the numbers of neurons and glial cells with minimum bias that is inherent in the counting procedures using conventional histology (Herculano-Houzel and Lent 2005). Their findings showed that primate brains have a larger number of neurons than rodent brains of similar size (Herculano-Houzel et al. 2007). They also revealed that the prefrontal region of both human and nonhuman primates holds about 8% of cortical neurons and the human prefrontal cortex is enlarged along the same allometric trajectory as for other primates (Gabi et al. 2016).

In volumetric studies, X-ray computed tomography (CT) provided accurate measurements of the skull, not only in extant species but also in fossils. Endocranial volumes thus could be analyzed with much greater accuracy than with classical methods. For soft tissue analysis, magnetic resonance imaging (MRI) can demarcate nervous tissues from cerebrospinal fluid, gray matter from white matter, and enables volume analysis of different modules of the nervous system, each involved in different cognitive functions.

Concerning the volumetric evaluation of the extant primate species, including humans, Semendeferi et al. (2002) conducted a series of studies that demonstrated striking commonalities among humans and other great apes. When gray matter volumes were compared, the human had the largest frontal lobes only in absolute terms, while the proportion of the frontal lobes to the total cortex is very similar in humans (37.7%) and other great apes (35.4% in chimpanzee). Gibbons (29.4%) and monkeys (30.6% in rhesus, 29.6% and 31.5% in capuchin) had significantly smaller frontal cortical volume than the great apes, but the difference was smaller than that in Brodmann's data (Brodmann 1912). Similarly, the proportion of the parieto-occipital sector in the human brain was not noteworthy. In contrast, the proportion of the temporal cortex was greater in humans than in other apes.

The similarity of the frontal proportion in great apes and humans seems to contradict Brodmann's findings. Semendeferi attributed the discrepancy to the small sample size of previous studies; however, one important difference needs to be pointed out. Brodmann measured the surface area of the cortex, while Semendeferi analyzed cortical volumes. Brodmann's data showed that the proportion of areas 4 and 6 dropped quite markedly in humans compared to the chimpanzee. Areas 4 and 6 are the thickest cortical areas in the primate brain, which contribute a lot in the volumetric comparisons, whereas the prefrontal areas are markedly thinner than areas 4 and 6 (Fig. 3.1). This means that in the volumetric analyses of the

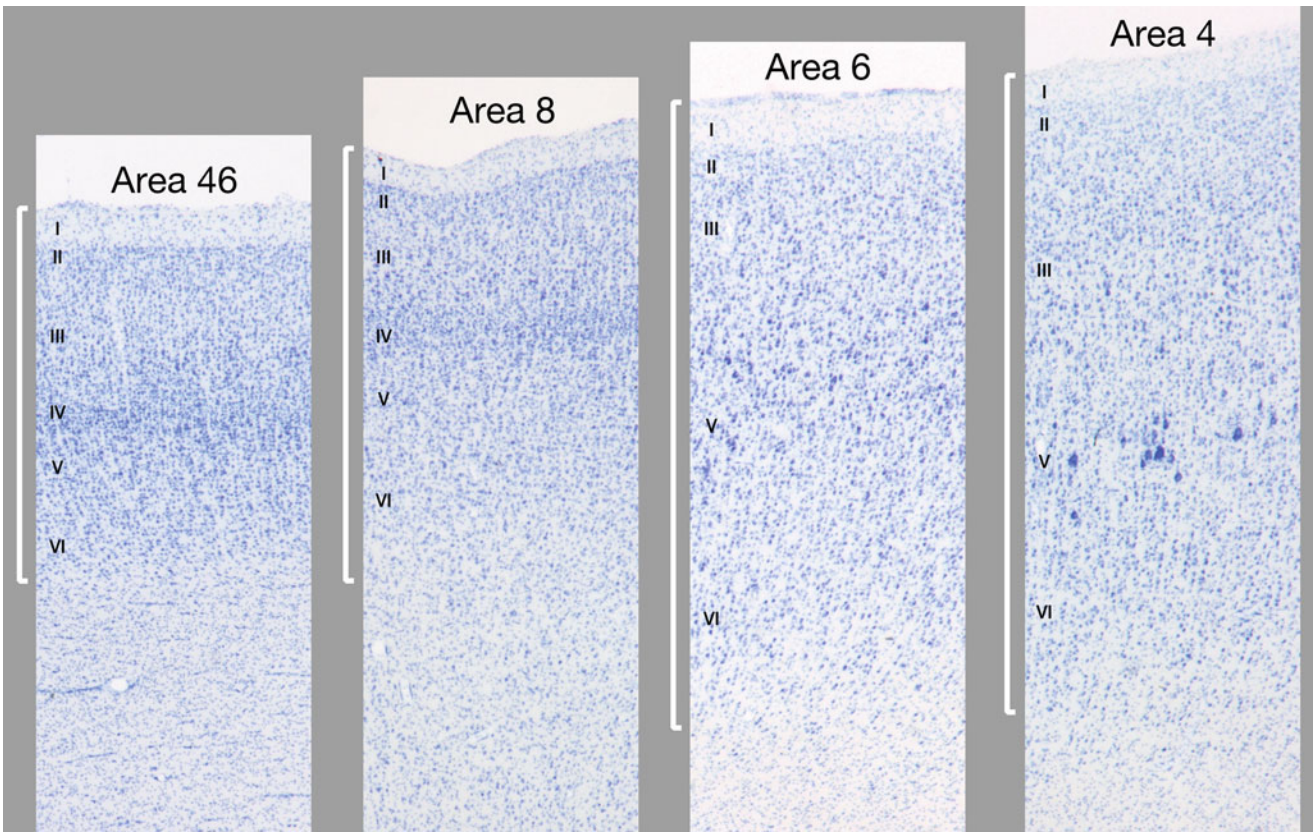

Fig. 3.1 Cortical structure of frontal areas in the macaque monkey. Sections were stained using the Nissl method for cytoarchitecture. Prefrontal areas (areas 46 and 8) are much thinner than premotor and primary motor areas (areas 6 and 4). *Roman numerals* represent the numbers of layers

frontal cortex, the expansion of the prefrontal areas may be partly masked by the relative decrease of areas 4 and 6 when we compare the proportion to the total cortical volume. The precentral cortical volume showed indeed a larger difference between humans and other great apes (28.8–33% in humans, 25.5–29.7% in other great apes) than the entire frontal cortical volume (Semendeferi et al. 2002), although the difference in the volumetric analysis remains smaller than in surface area analysis. A more recent study examining the prefrontal cortical volume in comparison with that of the primary visual cortex (striate cortex) demonstrated that the prefrontal/striate proportion in human is markedly enlarged compared to chimpanzee, while chimpanzee has also a larger value than macaque monkeys (Passingham and Smaers 2014).

Evolution of the nervous tissue does not affect the gray matter alone. The white matter that connects various regions of the cortex and subcortical nuclei also changes during the evolution. Schoenemann et al. (2005) differentiated volumes of gray matter and white matter using MRI and showed that the largest difference between human and nonhuman primates was the prefrontal white matter volume in proportion to the total cerebral white matter. The prefrontal white matter volume represented 10.9% of the total cerebral white matter in humans and 7.7% in the other great apes, whereas the proportion of prefrontal gray matter to the total cerebral gray matter showed a much smaller difference between humans and the other great apes (14.4% in human, 13.4% in great apes). These values need further refinement since the definition of the prefrontal sector in this study is not based on the cytoarchitecture but an approximation in which they define the level of the anterior tip of the genu of the corpus callosum as the caudal border of the prefrontal cortex. It can safely be concluded that the development of the prefrontal cortex comprises the increased cortical connections to and from other parts of the cortex and subcortical structures.

For this line of research, a study by Glasser and van Essen (2011) may open a possibility to more precise delineation of cortical areas based on MRI images. Using the ratio of signal intensities obtained in T1-weighted and T2-weighted images, they estimated the myelin content of the cortex and illustrated the borders between motor and somatosensory areas. In combination with this method, volumetric analysis using MRI will provide more detailed information of cortical areas of extant primate species including human.

3.4 Recent Advances in Neanderthal Paleoneurology

Concerning fossil hominids, we have to focus on the evolutionary changes of the brain that may affect the morphology of the skull. There is a long history of studies of the outer and inner structures of the skull. Recent computer-assisted reconstruction of the fossil skulls and imaging techniques, including CT and MRI, have brought about less-biased and statistically sophisticated tools in this field of research.

In the evolutionary differences between Neanderthals and modern humans, Bruner and his colleagues analyzed landmarks on the computer-reconstructed virtual endocasts of anatomically modern humans, Neanderthals, and more archaic hominines and demonstrated “parietal expansion” in modern humans compared with the Neanderthals and the other hominines (Bruner et al. 2003; Bruner 2004). The findings imply the possibility that modern humans obtained additional capacity in cognitive functions implemented in the parietal lobe, for example, visuospatial coordination and integration.

For the moment, it is reasonable to assume that parietal expansion resulted from increased cortical and white matter volume in the parietal lobe. However, there remains a possibility that expansion of other regions of the brain caused a secondary shift in the location of the parietal lobe. The net changes of the parietal volume therefore cannot be determined unless we (1) locate the border of the parietal lobe and (2) quantify the development of subcortical structures such as the basal ganglia and the diencephalon. The second factor is not a particular issue because of the relative stability of subcortical structures during hominid evolution. The first factor, however, needs to be examined given that a shift of the cortical borders has often occurred during evolution, for example, a caudal shift of the border of the primary visual area V1 (lunate sulcus on the lateral surface) has occurred since hominines differentiated from apes.

The same is true for the frontal lobe. Even if a significant change of the frontal lobe was not proven in terms of expansion or shrinkage from the center of the cerebral hemispheres, the frontal cortex may have been enlarged when the caudal border of the frontal lobe or the prefrontal cortex shifted caudally. Identifying the borders between cortical regions is thus a prerequisite for quantitative analysis of the proportional changes of different cortical regions. We have evaluated two approaches in tackling this issue, which we will describe in this chapter.

3.5 Two Approaches to Determine Borders of Cortical Regions

In fossil species, where it is not possible to identify regional borders based on the internal structures of the cortex, we have only limited means in approximating the borders. A widely adopted method is to use cerebral sulci as proxies of cortical borders. Some of the sulci are known to correspond to borders of cortical areas, particularly to borders between major cortical areas that are well preserved during evolution: the Sylvian fissure between the frontal and parietal lobes superiorly and the temporal lobe inferiorly, the central sulcus between the primary motor area (M1) and the primary

somatosensory area (SI), the postcentral sulcus between SI and the posterior parietal lobe, the intraparietal sulcus between the superior and inferior parietal lobules, and the lunate sulcus demarcating the rostral border of the primary visual area (V1). Other sulci are also useful to identify the location of some cortical areas because they contain those areas, for example, the calcarine sulcus for V1, the inferior frontal sulcus or principal sulcus for area 46, and the intraparietal sulcus for anterior, lateral, medial, and ventral intraparietal areas (areas AIP, LIP, MIP, and VIP).

Recent advances in geometric morphometrics provided a statistically secure approach to evaluate the morphology of fossil skulls. On the other hand, we cannot determine the extent of cortical areas directly from skulls in fossil species. We need to know the relationship between skull landmarks and the cortical borders before inferring the extent of an area.

The abovementioned sulci often leave ridges, and adjacent gyri leave imprints or depressions on the inner surface of the skull. On the endocast of the skull, therefore, we can observe the convolutional patterns of the cortical surface. In cases where we can observe those patterns, we can identify the major sulci and gyri on the endocast without depending on indirect inferences. The major difficulty in this approach is that the convolutional patterns are not obvious in all primate species.

Another approach is to infer the locations of sulci using skull landmarks such as sutures, glabella, bregma, lambda, inion, pterion, and asterion. Although causal relationships between landmarks and cerebral structures are not biologically confirmed, these landmarks are robust and can be identified in many fossil skulls.

3.6 Locating Cerebral Sulci Based on Endocast Surface Morphology

This first approach has been used for fossil skulls since the early ages of fossil hominine research. Boule and Anthony (1911) illustrated almost the entire extent of the lateral sulcus, portions of the orbital, superior and middle frontal, postcentral, external parieto-occipital, superior temporal, lunate, and calcarine sulci on the endocast of La Chapelle-aux-Saints. Anthony (1913) described imprints of major sulci including some portions of the lateral sulcus; the superior, middle, and inferior frontal sulci; the postcentral sulcus; the intraparietal sulcus; and the parieto-occipital and lunate sulci on the endocast of La Quina.

In terms of the validity of those inferences, Symington (1916) criticized the simple assumption of the correspondence of endocranial morphology to cerebral convolutions and stated that "the simplicity or complexity of the cerebral fissures and convolutions cannot be determined with any degree of accuracy from endocranial casts." Le Gros Clarke et al. (1936) compared endocasts of chimpanzees with the brains derived from the same individual and pointed out the risk in using endocranial depressions to identify cerebral sulci, particularly in the parietal area. Ogawa et al. (1970) confirmed Symington's concerns in their study on the Amud endocast. Smith-Agreda (1955) examined more than 300 modern human skulls and reported that impressions representing cerebral gyri were observed typically in the anterior and middle cranial fossa, and the correspondence was less secure on the inner surface of the lateral wall of the skull. Only in a few abnormal cases were the convolutional patterns clearly observed up to the vertex. These findings indicate that the inference of the cerebral gyri and sulci using the skull may be reliable in the basal portion of the skull but is increasingly difficult toward the vertex.

On the other hand, endocasts of smaller primate skulls usually show marked convolutional patterns that apparently correspond to cerebral sulci and gyri. Le Gros Clarke (1945) estimated the convolutional pattern of the cerebral cortex using endocasts in fossil lemuroids. Radinsky (1972) reviewed the taxonomic characteristics of endocasts of monkeys and presented some data on the sulci observed on the endocasts. A recent study on fossil cercopithecoid skulls also showed marked imprints on the endocasts that apparently corresponded to the major sulci on the brain (Beaudet et al. 2016). Even in hominines, an *Australopithecus*, Taung Child, exhibited imprints that closely resembled cerebral sulci and gyri (Dart 1925, 1940). However, identification of sulci is not always unambiguous (for discussion concerning the lunate sulcus, see papers by Falk (1980, 1983) and Holloway (Holloway 1980)). The most problematic issue is that it is impossible to evaluate the reliability of the inference in fossil species.

To evaluate this approach, we first compared macaque monkey skulls with brains derived from the same animals (Kobayashi et al. 2014a). Figure 3.2 shows the skull and brain of a crab-eating macaque. In all the examined endocasts, we clearly identified depressions corresponding to the principal, arcuate, central, intraparietal, lunate, lateral, superior temporal, anterior middle temporal, medial, and lateral orbital sulci. We also observed very shallow indentations, for instance, the superior precentral and postcentral dimples. Even individual differences in the course of some sulci were confirmed on the endocast, for example, in the lower end of the central sulcus and connections between the medial and lateral orbital sulci.

We next analyzed dry skull specimens that were stored at the National Defense Medical College for educational purposes (Table 3.2). We scanned the skulls using an Asterion CT scanner (Toshiba; Tokyo, Japan) and obtained full three-dimensional image stacks consisting of 253–281 contiguous, 0.5-mm-thick slices. The images consisted of a 512 × 512 pixel matrix, with a pixel size of 0.351 × 0.351 mm. CT

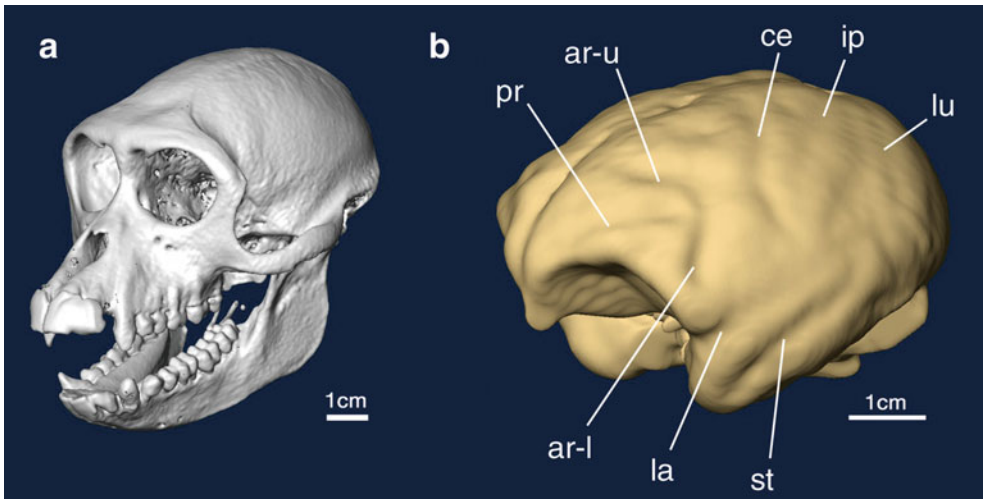

Fig. 3.2 A skull (**a**) and a virtual endocast (**b**) of a crab-eating monkey specimen reconstructed from CT data. *ar-l*, *ar-u* lower/upper limb of arcuate sulcus, *ce* central sulcus, *ip* intraparietal sulcus, *la* lateral sulcus, *lu* lunate sulcus, *pr* principal sulcus, *st* superior temporal sulcus

Table 3.2 Sulci identified on endocasts of dry skull specimen

	pr	ar	sf	fo	ipc	spc/spd	ce	ip	lu	la	st	amt	ot	o	lo	mo	CS
Lemur catta	○						○	○		○	○		○				—
Alouatta	○						○	○	○	○	○	○		○			+
Presbytis cristata 1	○	○					○	○		○	○	○			○	○	—
Presbytis cristata 2	○	○					○	○	○	○	○	○			○	○	+
Presbytis cristata 3	○	○					○	○		○	○	○			○	○	—
Lagothrix 1	○		○		○	○	○	○	○	○	○	○			○	○	+
Lagothrix 2	○		○		○	○	○	○	○	○	○	○			○	○	+
Pygathrix nemaeus	○	○				○	○	○	○	○	○	○			○	○	+
Macaca arctoides 1	○	○				○	○	○	○	○	○	○			○	○	+
Macaca arctoides 2	○	○				○	○		○	○	○	○			○	○	+
Macaca fascicularis 1	○	○				○	○	○	○	○	○	○			○	○	+
Macaca fascicularis 2	○	○				○	○	○	○	○	○	○			○	○	±
Macaca fuscata 1	○	○				○	○		○	○	○	○			○	○	+
Macaca fuscata 2	○	○				○	○		○	○	○	○			○	○	+
Hylobates	○		○	○	○	○	○	○	○	○	○		○		○	○	+
Pan troglodytes										○					○	○	+

images were analyzed using the Amira 5.4 software package (Visage Imaging; Berlin, Germany) on a Z620 workstation (Hewlett-Packard Japan; Tokyo, Japan) on a Mac Pro computer (Apple; Cupertino, CA, USA). To create virtual endocasts, we selected pixels inside the skull in each slice based on their density and reconstructed the surfaces. Cerebral sulci were identified based on our macroscopic samples of monkey brains for crab-eating macaques, Japanese macaques, and chimpanzees, as well as using descriptions in previous reports (Connolly 1936; Connolly 1950; Paxinos et al. 2000; Bailey et al. 1950).

Table 3.2 also shows the cerebral sulci identified on the endocasts. The skull of the chimpanzee was opened, so that we could get an incomplete reconstruction of the endocast. In monkeys and a gibbon, we observed the major cerebral sulci that faced the inner surface of the skull (Fig. 3.3). As for the sulci demarcating cerebral lobes, the lateral sulcus (la) and the central sulcus (ce; Rolando fissure) were clearly observed in all the skulls. In the frontal lobe, sulci observed in all cases included the principal sulcus (pr), which is homologous to the inferior frontal sulcus in human, and the upper and lower limbs of the arcuate sulcus (ar), which correspond to the superior frontal sulcus (sf) and the inferior precentral sulcus (ipc), respectively. The medial and lateral orbital sulci (mo, lo) were seen in a gibbon and monkeys, except for the lemur and the howler monkey, the latter having only a single orbital sulcus (o). In the parietal lobe, the intraparietal sulcus (ip) was identified in all the skulls except for two Japanese macaque specimens, which had the largest skulls among the monkeys we examined. In the Japanese macaques, the parietal lobe was so smooth that hardly any trace of sulci was detected; the central sulcus was

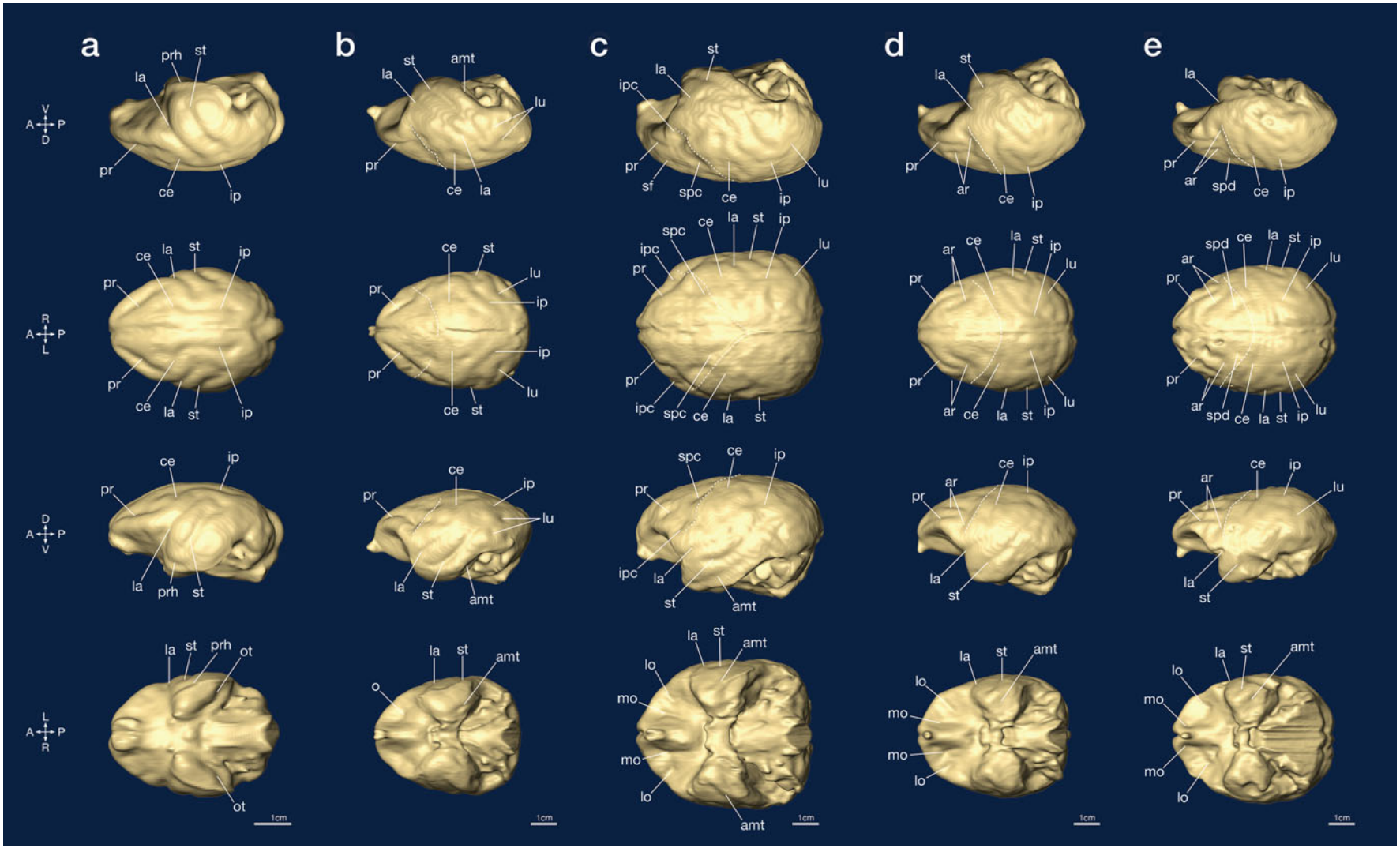

Fig. 3.3 Virtual endocasts reconstructed from dry skull specimens. (**a**) Lemur (*Lemur catta*), (**b**) howler monkey (*Alouatta*), (**c**) woolly monkey (*Lagothrix*) 2, (**d**) silvered leaf monkey (*Presbytis cristata*) 2, (**e**) douc (*Pygathrix nemaeus*), (**f**) *red*-faced stump-tailed macaque (*Macaca arctoides*) 1, (**g**) crab-eating macaque (*Macaca fascicularis*) 2, (**h**, **i**) Japanese macaque (*Macaca fuscata*) 1–2, (**j**) gibbon (*Hylobates*). *Top*, *middle-top*, *middle-bottom*, and *bottom* panels show the *right lateral*, *top*, *left lateral*, and *bottom* sides of the endocasts, respectively. A scale bar represents 1 cm for each specimen. *amt* anterior middle temporal sulcus, *ar* arcuate sulcus, *ce* central sulcus, *fo* fronto-orbital sulcus, *ip* intraparietal sulcus, *ipc* inferior precentral sulcus, *la* lateral sulcus, *lo* lateral orbital sulcus, *lu* lunate sulcus, *mo* medial orbital sulcus, *o* orbital sulcus, *ot* occipitotemporal sulcus, *pr* principal sulcus, *prh* posterior rhinal sulcus, *sf* superior frontal sulcus, *spc* superior precentral sulcus, *spd* superior precentral dimple, *st* superior temporal sulcus

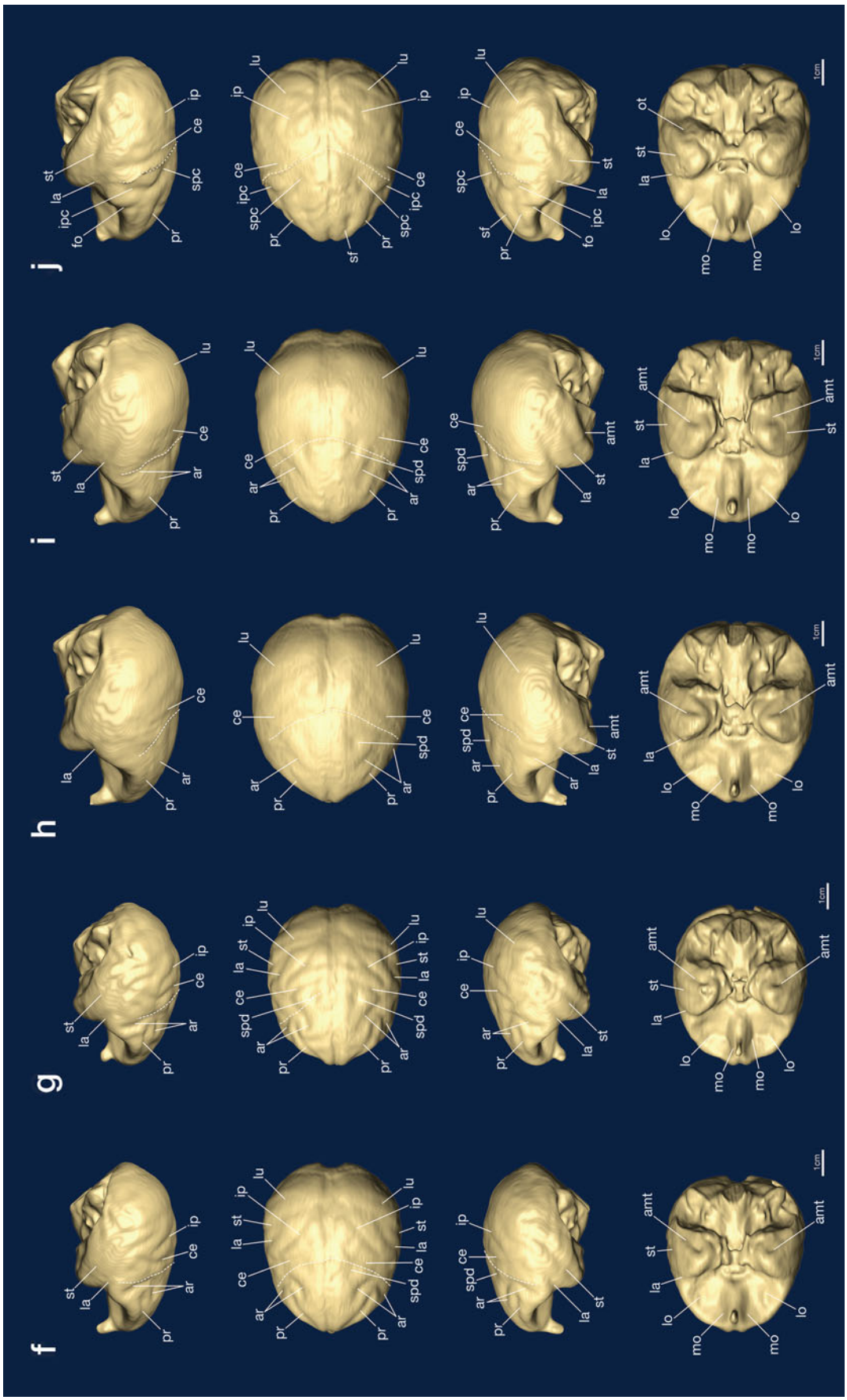

Fig. 3.3 (continued)

less distinct than in other monkeys. In the occipital lobe, the lunate sulcus (lu) was observed in most of the skulls, although very faintly in the Japanese macaques. In the temporal lobe, the superior temporal sulcus (st) was most distinct in its anterior portion but obscured posteriorly in most of the endocasts. The anterior middle temporal sulcus (amt) was also found in most of the cases. We cannot deduce a general rule from the limited number of cases analyzed in the study above, but imprints on the endocasts will be highly informative in monkeys and lesser apes.

In humans and the other great apes, the inference of the location of cerebral sulci is more problematic. Our preliminary study in human infants showed convolutional patterns not only on the basal part but also on the vault of the endocast, although correspondence to cerebral sulci was not always clear (Matsui and Kobayashi 2012). The connective tissues and blood vessels on the brain surface are thinner in young animals. The major factors that seem to obscure the course of sulci are (1) the thick connective tissue and cistern around the anterior portion of the lateral sulcus and (2) the superior, inferior, and superficial middle cerebral veins that are often located on cerebral sulci. In addition, developing brains may exert more influence on the adjacent skull to make extra space in which to grow. Infant skulls may provide a clue in locating cerebral sulci on endocasts in species with large brains and skulls. Several major cerebral sulci were actually identified on the endocast of a child skull of Mojokerto (Balzeau et al. 2005). Developmental studies will be necessary to further evaluate this approach.

Another important issue is the deformation and fragmentation of skulls during fossilization process. Virtual reconstruction of the skulls on computers provides practical and useful tools for endocast analysis (for review, see Zollikofer 2002; Gunz et al. 2009; Ogihara et al. 2015). For example, in our project "Replacement of Neanderthals by Modern Humans" (http://www.koutaigeki.org/eng/index.html), we have also carried out research on the statistical interpolation of the missing parts of the skull (Kikuchi and Ogihara 2013; Amano et al. 2014, 2015) and on the assessment of the left-right asymmetry after elimination of the deformity of the original skull (Kondo et al. 2014). These methods will provide a less-biased reconstruction of skulls and contribute not only to the better estimation of the overall dimensions of endocasts but also to the more accurate reproduction of their surface morphology.

3.7 Inferring Cerebral Sulci Based on Skull Landmarks

This approach was not originally adopted for studies on fossil species but for neurological and neurosurgical needs before the development of radiological imaging techniques. A large number of studies were carried out since Broca's description on the spatial relationship between the central sulcus and the coronal suture (Broca 1861) (see review by Broca (1876) and Anderson and Makins (1889b)). For example, Horsley (1892) measured the location of the upper end of the central sulcus in the sagittal arch from glabella to inion; the central sulcus was located 12.5 mm posterior from the midpoint of the sagittal arch, which corresponded to 55.7% of the glabella – inion distance. Anderson and Makins (1889a) also reported that the upper end of the central sulcus fell between the midsagittal point and 19 mm posterior from it. Cunningham and Horsley (1892) conducted a more elaborated analysis and stated that the central and precentral sulci were "remarkably constant in its relative position to the rest of the hemisphere."

Interestingly, Cunningham and Horsley (1892) showed illustrations of the dissected heads of humans and nonhuman primates, in which the frontal and parietal bones, as well as the squamous parts of the temporal and occipital bones, were largely removed except for the portions adjacent to the sutures (Fig. 3.4). In nonhuman primates (rhesus, baboon, cebus, orangutan, and chimpanzee), the inferior precentral sulcus, or its homologue, the lower limb of the arcuate sulcus, was largely hidden underneath the bones comprising the coronal suture, while in humans the inferior precentral sulcus was located posteriorly, some distance from the suture. Flatau and Jacobsohn (1899) also illustrated the cerebral convolutional pattern with the skull and certain sutures in a lemur, macaque monkey, and chimpanzee (Fig. 3.5). The lower portion of the coronal suture fell over the position of the inferior precentral sulcus in the chimpanzee and the lower arcuate sulcus in the macaque.

These findings prompted us to reevaluate the relationship between the sulci and sutures. We first utilized the skulls and brains of five *Macaca fascicularis* monkeys. We examined and compared the locations of the coronal suture and the lower limb of the arcuate sulcus (Kobayashi et al. 2014b). The coronal suture was identified on CT images as curved low-density lines extending laterally from the bregma. The arcuate sulcus was traced on lateral photographic images of the brain and was superimposed on the CT images of the skull. In this study, we defined the plane through the frontal and occipital poles as horizontal and measured the horizontal distance of the suture and the sulcus from the frontal pole at different dorsoventral levels (from level 0 at the fronto-occipital line through level 10 at the vertex of the brain (Fig. 3.6). The distances were normalized by using their proportions to the fronto-occipital length of the endocast. The data showed that the lower limb of the arcuate sulcus was located slightly anterior to the lower half of the coronal suture within a very limited area: the average distance ± S.D. was 0.0–1.4% ± 1.1–3.0% of the distance between the frontal and occipital poles.

We next analyzed the dry skull specimens used for the evaluation of the first approach (examples are shown in Fig. 3.3). The suture was fused completely and left no trace of the coronal suture in the lemur and two of the silvered leaf monkey specimens and was partially obscured in a crab-

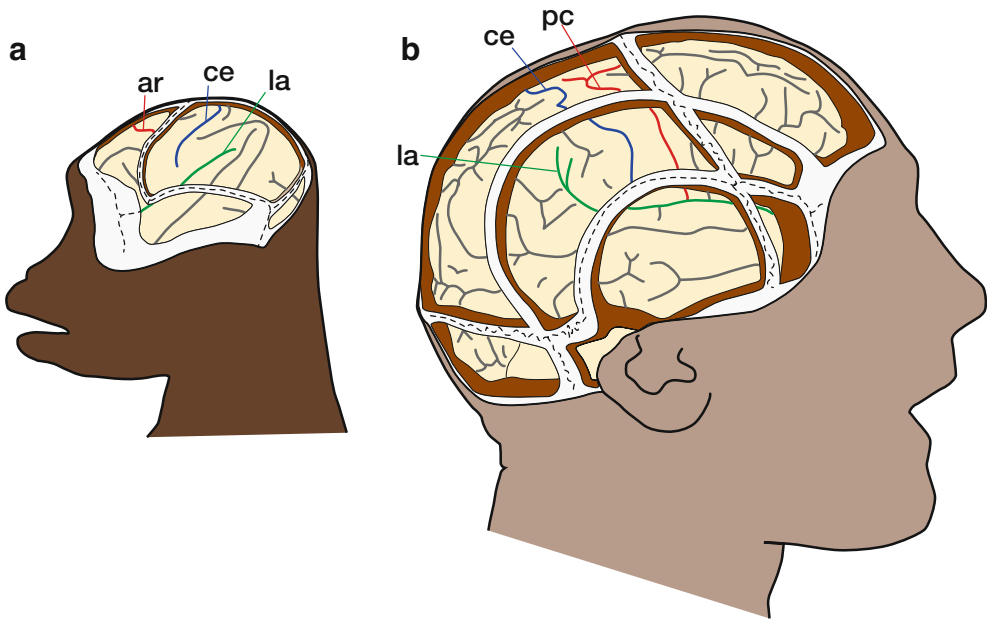

Fig. 3.4 Spatial relationship between sutures and cerebral sulci in rhesus monkey (**a**) and human (**b**) illustrated by Cunningham (Redrawn from Cunningham and Horsley 1892). *ar* arcuate sulcus (upper limb), *ce* central sulcus, *la* lateral sulcus, *pc* precentral sulcus. Note that bones adjacent to the temporal ridge remained in (**a**)

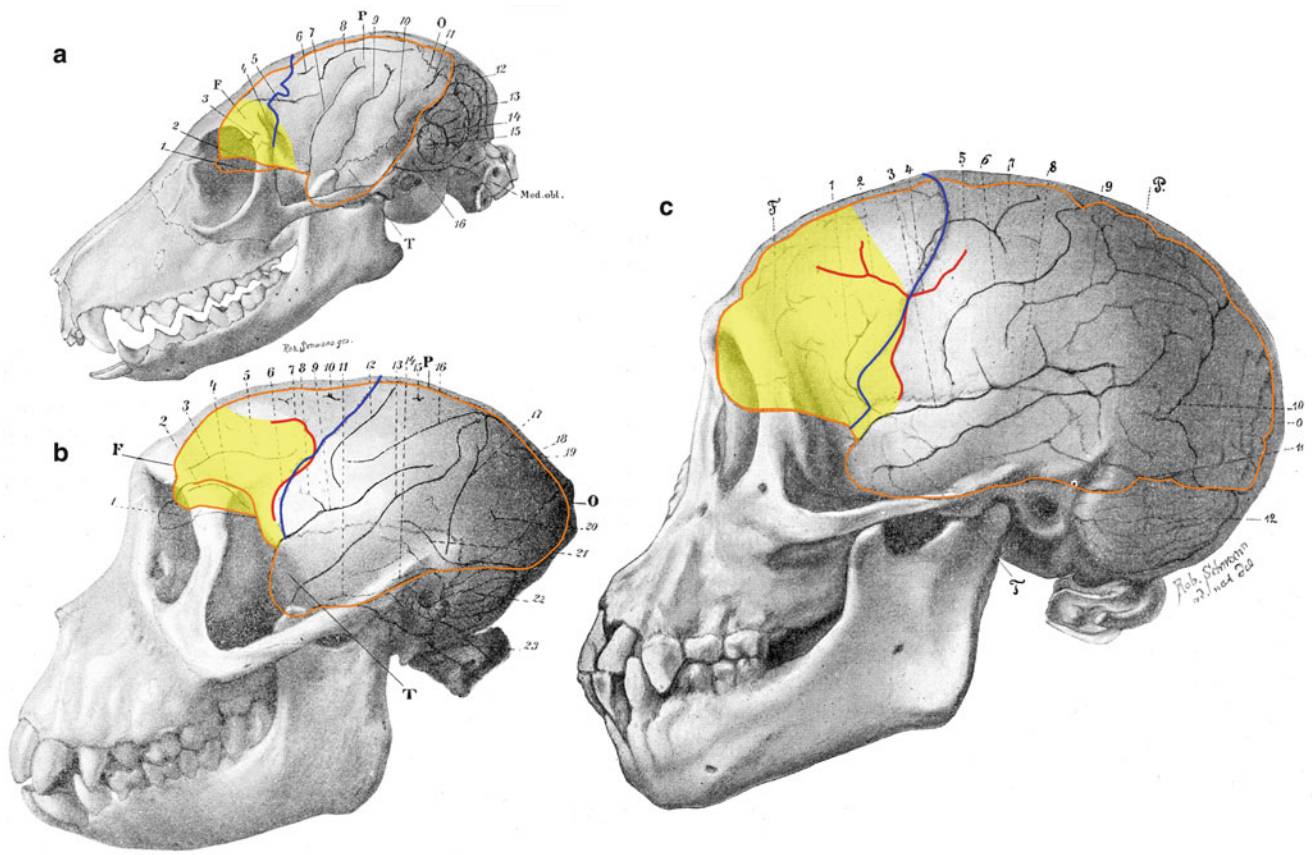

Fig. 3.5 Spatial relationship between sutures and cerebral sulci in lemur (**a**), rhesus monkey (**b**), and chimpanzee (**c**), illustrated by Flatau and Jacobsohn (1899). Color was added to the original picture. *Blue lines* and *red lines* represent the coronal suture and the arcuate sulcus/inferior precentral sulcus, respectively. Areas painted in yellow depict the prefrontal cortex determined in later studies

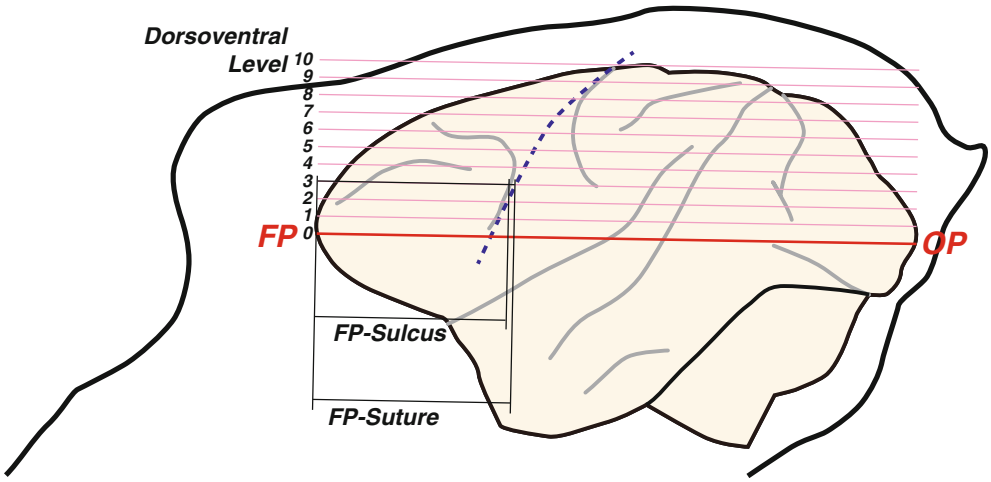

Fig. 3.6 Measurements of the locations of the coronal suture and the arcuate sulcus. We defined the line connecting the frontal and occipital poles (FP, OP) as the horizontal line. The space between the horizontal line and the vertex of the brain was divided by nine lines with equal intervals. We determined the relative dorsoventral levels: from DV0 on the horizontal line to DV10 on the line through the vertex and measured the horizontal distance of the suture and the sulcus from the frontal pole. To normalize between species and individual differences of the skull and brain size, we used the ratio of the distance to the fronto-occipital length (FP-OP)

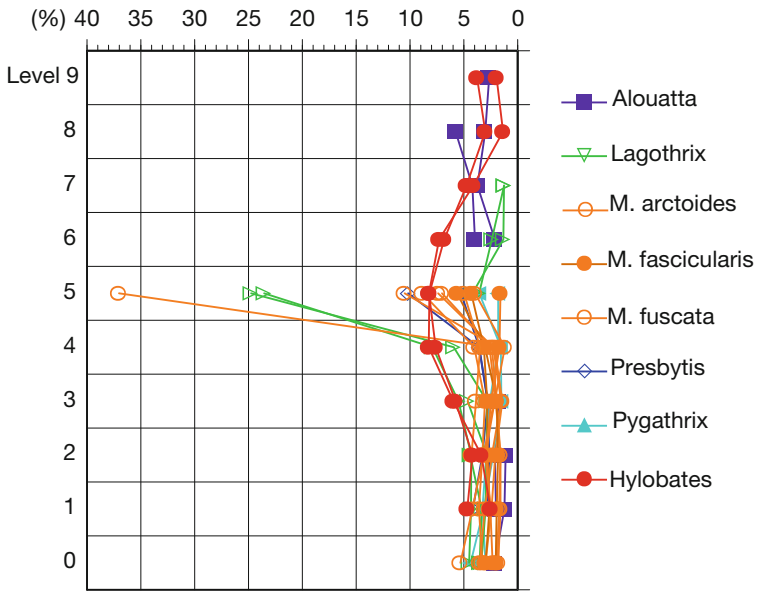

Fig. 3.7 Distance of the arcuate or precentral sulcus from the coronal suture. In dry skulls, sutures were easily identified as sharp, thin ridges on the endocasts in contrast to smooth, wide bumps corresponding to cerebral gyri. The *horizontal axis* of the graph is for the distance from the coronal suture in proportion to the fronto-occipital length (in percentage), and the vertical axis is for the dorsoventral levels as indicated in Fig. 3.6. The *right edge* indicates the location of the coronal suture, and the *left side* is anterior. *Colored lines* represent the locations of the sulci; different species are shown with different markers

eating macaque specimen. In other skulls, however, the coronal suture was easily identified, both on CT images and on the reconstructed endocasts. At dorsoventral levels 0–1, the arcuate sulcus was often absent or obscured due to the proximity of the lateral sulcus. At levels 2–4, the suture and sulcus were clearly and most frequently observed on the endocasts. At level 5, the arcuate sulcus made a sharp curve anteriorly to form its upper limb and ended between levels 5 and 6 except in the howler monkey and the gibbon. Even though the samples were derived from a wide variety of taxa, the lower limb of the arcuate sulcus or the inferior precentral sulcus was generally located slightly anterior to the lower half of the coronal suture with an amazingly small variance at levels below 4 (Fig. 3.7). The location of the lower half of the coronal suture and the lower limb of the arcuate sulcus exhibited strong correlation at levels 2–3 (Fig. 3.8a).

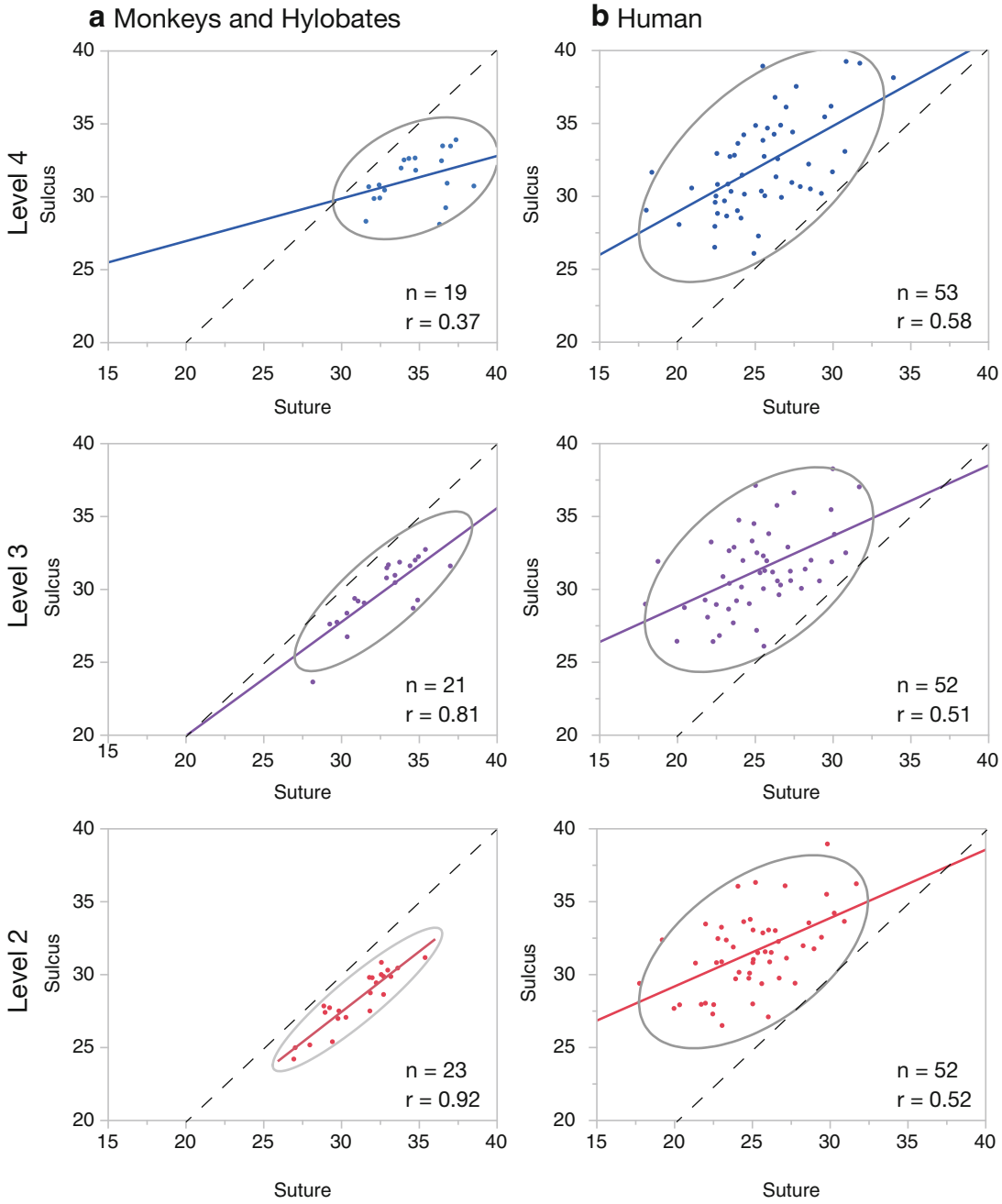

Fig. 3.8 Correlation of the locations of the coronal suture and the arcuate sulcus/inferior precentral sulcus. In dry skull specimens of monkeys and a gibbon (**a**), the locations of the suture and arcuate sulcus show strong correlation at dorsoventral levels 2–3 and moderately strong correlation at level 4, where the sulcus bends anteriorly in several samples. In human cadavers (**b**), the location of the suture exhibited moderately strong correlations at levels 2–4. The regression line and the 95% probability ellipse are drawn in each scatter plot

A similar correlation was also observed in the human, in which we measured the location of the suture on the inner surface of the skull and that of the sulcus on the brain in Japanese cadavers. It should be noted that the individual differences were even larger in humans than in primate samples from different taxa (Fig. 3.8b). However, the location of the coronal suture and the inferior precentral sulcus showed moderately strong correlations, which indicate that, solely based on a skull, we may be able to infer the location of the precentral sulcus of the same individual. We plan to increase the number of the analyzed cases to establish a statistically verified method to infer the location of the inferior precentral sulcus and apply it to Neanderthal skulls.

Recently, the extent of the precuneus, which is highly variable in the human, was statistically analyzed using MRI (Bruner et al. 2015b) and compared with the extent of the parietal bone (Bruner et al. 2015a). The results showed low correlation between the parietal lobe and parietal bone lengths ($r = 0.27$ for chords and 0.32 for arcs) and between the precuneus length and the parietal bone length ($r = 0.20$ for chords and 0.24 for arcs). Both correlations are considerably lower than those observed between the locations of the coronal suture and the inferior precentral sulcus in our study. The reason of this discrepancy is not clear, but one possible factor is that bregma and lambda are formed by the fusion of the concentric ossification of the frontal, parietal, and occipital bones long after birth, and their positions can be modified by differences in ossification speed between adjacent bones. The lateral aspect of the coronal suture is fused earlier and might be more stable than the locations of bregma and lambda. A comprehensive analysis of the individual differences of subdivisions of the brain and the skull will be necessary to evaluate the validity of the use of skull landmarks as reference points to infer borders of brain regions.

3.8 Concluding Remarks

In this article, we have summarized classical and recent views concerning the cortical evolution in primates including human and also presented two approaches we examined recently to infer the extent of cortical areas based on the skull morphology.

The method using the endocast surface morphology is more straightforward and useful in monkeys and gibbons which have relatively smaller skulls and may be also applicable to very young individuals in greater apes and humans. However, probably due to the thickness of connective tissue and the vascularity, it is not suitable in adult humans except for the lower portion of the cortex, such as the orbitofrontal and inferior temporal cortices.

The other method using the coronal suture as a landmark to infer the location of the precentral sulcus can be applied in any skull unless the suture is fused by ossification. This approach is, however, based on an assumption that the relationship between the locations of the suture and the sulcus is stable in different species. Because the relationship in the modern human is different from that in monkeys and gibbons, further studies in the extant great apes will be necessary before we interpolate it in fossil hominines.

Acknowledgment The authors thank Ms. Mayumi Watanabe, Mr. Tohru Tamai, and Mr. Hiroshi Sasaki at the Department of Anatomy and Neurobiology, National Defense Medical College, for the assistance in histology and cadaver analysis. This study was supported by Grant-in-Aid for Scientific Research on Innovative Areas (Grant No. 23101509, 25101711) from the Japanese Ministry of Education, Science, Culture, and Technology.

References

Amano H, Morita Y, Nagano H, Kondo O, Suzuki H, Nakatsukasa M, Ogihara N (2014) Statistical interpolation of missing parts in human crania using regularized multivariate linear regression analysis. In: Dynamics of learning in neanderthals and modern humans, vol 2. Springer, pp 161–169

Amano H, Kikuchi T, Morita Y, Kondo O, Suzuki H, Ponce de León MS, Zollikofer CP, Bastir M, Stringer C, Ogihara N (2015) Virtual reconstruction of the Neanderthal Amud 1 cranium. Am J Phys Anthropol 158(2):185–197

Anderson W, Makins GH (1889a) Experiments in Cranio-cerebral topography. J Anat Physiol 23(Pt 3):455–465

Anderson W, Makins GH (1889b) Experiments in Cranio-cerebral topography. Lancet 2:61–64

Anthony R (1913) L'encéphale de l'homme fossile de La Quina. Bull Mém Soc d'Anthropol Paris:117–194

Ariëns Kappers CU (1909) The phylogenesis of the palaeo-cortex and archi-cortex compared with the evolution of the visual neo-cortex. Arch Neurol Psychiatr 4:161–173

Bailey P, von Bonin G, McCulloch WS (1950) The isocortex of the chimpanzee. The University of Illinois Press, Urbana

Balzeau A, Grimaud-Herve D, Jacob T (2005) Internal cranial features of the Mojokerto child fossil (East Java, Indonesia). J Hum Evol 48 (6):535–553

Beaudet A, Dumoncel J, de Beer F, Duployer B, Durrleman S, Gilissen E, Hoffman J, Tenailleau C, Thackeray JF, Braga J (2016) Morphoarchitectural variation in South African fossil cercopithecoid endocasts. J Hum Evol 101:65–78

Blinkov SM, Glezer IaI (1968) The human brain in figures and tables: a quantitative handbook. Basic Books, New York

Boule M, Anthony R (1911) L'encéphale de l'homme fossile de la Chapelle-aux-Saints. Anthropologie 22:129–196

Broca P (1861) Remarques sur le siége de la faculté du langage articulé, suivies d'une observation d'aphémie (perte de la parole). Bull Soc Anat 2e Ser 6:330–357

Broca P (1876) Sur la topographie cranio-cérébrale ou sur les rapports anatomiques du crane et du cerveau. Revue d'Anthroplogique:193–248

Brodmann K (1906) Beiträge zur histologischen Lokalisation der Grosshirnrinde. Fünfte Mitteilung: Über den allgemeinen Bauplan des Cortex pallii bei den Mammaliern und zwei homologe Rindenfelder im besonderen. Zugleich ein Beitrag zur Furchenlehre. J Psychol Neurol 6(Ergänzungsheft):275

Brodmann K (1912) Neue Ergebnisse über die vergleichende histologische Lokalisation der Grosshirnrinde mit besonderer Berücksichtigung des Stirnhirns. Anat Anz 41:157–216

Bruner E (2004) Geometric morphometrics and paleoneurology: brain shape evolution in the genus homo. J Hum Evol 47(5):279–303

Bruner E, Manzi G, Arsuaga JL (2003) Encephalization and allometric trajectories in the genus homo: evidence from the Neandertal and modern lineages. Proc Natl Acad Sci U S A 100(26):15335–15340

Bruner E, Amano H, de la Cuetara JM, Ogihara N (2015a) The brain and the braincase: a spatial analysis on the midsagittal profile in adult humans. J Anat 227(3):268–276

Bruner E, Roman FJ, de la Cuetara JM, Martin-Loeches M, Colom R (2015b) Cortical surface area and cortical thickness in the precuneus of adult humans. Neuroscience 286:345–352

Connolly CJ (1936) The fissural pattern of the primate brain. Am J Phys Anthropol 21(3):301–422

Connolly CJ (1950) External morphology of the primate brain. Thomas, Springfield

Cunningham DJ, Horsley V (1892) Contribution to the surface anatomy of the cerebral hemispheres: with a chapter upon Cranio-cerebral topography. Academy House, Dublin

Dart RA (1925) Australopithecus africanus: the man-ape of South Africa. Nature 115(2884):195–199

Dart RA (1940) The status of Australopithecus. Am J Phys Anthropol 26(1):167–186
Falk D (1980) A reanalysis of the South African australopithecine natural endocasts. Am J Phys Anthropol 53(4):525–539
Falk D (1983) The Taung endocast: a reply to Holloway. Am J Phys Anthropol 60(4):479–489
Flatau E, Jacobsohn L (1899) Handbuch der Anatomie und vergleichenden Anatomie des Centralnervensystem der Säugetiere. 1. Makroskopischer Teil. Karger, Berlin
Flechsig P (1920) Anatomie des menschlichen Gehirns und Rückenmarks auf myelogenetischer Grundlage. Thieme, Leipzig
Gabi M, Neves K, Masseron C, Ribeiro PF, Ventura-Antunes L, Torres L, Mota B, Kaas JH, Herculano-Houzel S (2016) No relative expansion of the number of prefrontal neurons in primate and human evolution. Proc Natl Acad Sci U S A 113(34):9617–9622
Gibson KR, Rumbaugh D, Beran M (2001) Bigger is better: primate brain size in relationship to cognition. In: Evolutionary anatomy of the primate cerebral cortex. Cambridge University Press, Cambridge, pp 79–97
Glasser MF, Van Essen DC (2011) Mapping human cortical areas in vivo based on myelin content as revealed by T1- and T2-weighted MRI. J Neurosci 31(32):11597–11616
Gunz P, Mitteroecker P, Neubauer S, Weber GW, Bookstein FL (2009) Principles for the virtual reconstruction of hominin crania. J Hum Evol 57(1):48–62
Herculano-Houzel S, Lent R (2005) Isotropic fractionator: a simple, rapid method for the quantification of total cell and neuron numbers in the brain. J Neurosci 25(10):2518–2521
Herculano-Houzel S, Collins CE, Wong P, Kaas JH (2007) Cellular scaling rules for primate brains. Proc Natl Acad Sci U S A 104 (9):3562–3567
Holloway RL (1980) Revisiting the south African Taung australopithecine endocast: the position of the lunate sulcus as determined by the stereoplotting technique. Am J Phys Anthropol 56(1):43–58
Horsley V (1892) On the topographical relations of the cranium and surface of the cerebrum. In: Topography CttSAotCHWaCUC-c (ed) Contribution to the surface anatomy of the cerebral hemispheres: with a chapter upon Cranio-cerebral topography. Academy house, Dublin, pp 306–358
Jerison HJ (1973) Evolution of the brain and intelligence. Academic, New York
Kikuchi T, Ogihara N (2013) Computerized assembly of neurocranial fragments based on surface extrapolation. Anthropol Sci 121 (2):115–122
Kobayashi Y, Matsui T, Haizuka Y, Ogihara N, Hirai N, Matsumura G (2014a) Cerebral sulci and gyri observed on macaque endocasts. In: Dynamics of learning in neanderthals and modern humans, vol 2. Springer, pp 131–137
Kobayashi Y, Matsui T, Haizuka Y, Ogihara N, Hirai N, Matsumura G (2014b) The coronal suture as an indicator of the caudal border of the macaque monkey prefrontal cortex. In: Dynamics of learning in neanderthals and modern humans, vol 2. Springer, pp 139–143
Kondo O, Kubo D, Suzuki H, Ogihara N (2014) Virtual endocast of Qafzeh 9: a preliminary assessment of right-left asymmetry. In: Dynamics of learning in neanderthals and modern humans, vol 2. Springer, pp 183–190
Le Gros Clark WE (1945) Note on the palaeontology of the lemuroid brain. J Anat 79(Pt 3):123–126
Le Gros Clark WE, Cooper DM, Zuckerman S (1936) The endocranial cast of the chimpanzee. J R Anthropol Inst G B Irel 66:249–268
Matsui T, Kobayashi Y (2012) Developing cranial parameters that delineate subdivisions of the brain – skulls of human infants. Paper presented at the The 5th conference on replacement of Neanderthals by modern humans: testing evolutionary models of learning, Tokyo, April 14–16, 2012
Ogawa T, Kamiya T, Sakai S, Hosokawa H (1970) Some observation on the endocranial cast of the Amud man. In: Suzuki H, Takai F (eds) The Amud man and his cave site. The University of Tokyo Press, Tokyo, pp 411–424
Ogihara N, Amano H, Kikuchi T, Morita Y, Hasegawa K, Kochiyama T, Tanabe HC (2015) Towards digital reconstruction of fossil crania and brain morphology. Anthropol Sci 123 (1):57–68
Passingham RE, Smaers JB (2014) Is the prefrontal cortex especially enlarged in the human brain allometric relations and remapping factors. Brain Behav Evol 84(2):156–166
Paxinos G, Huang XF, Toga AW (2000) The rhesus monkey brain in stereotaxic coordinates. Academic, San Diego
Radinsky L (1972) Endocasts and studies of primate brain evolution. The functional and evolutionary biology of primates, ed R Tuttle Aldine[DF]
Schoenemann PT, Sheehan MJ, Glotzer LD (2005) Prefrontal white matter volume is disproportionately larger in humans than in other primates. Nat Neurosci 8(2):242–252
Semendeferi K, Lu A, Schenker N, Damasio H (2002) Humans and great apes share a large frontal cortex. Nat Neurosci 5(3):272–276
Smith-Agreda V (1955) The distribution of the impressions gyrorum at the inner side of the human cranium; with utilization of endocranial casts. Dtsch Z Nervenheilkd 173(1):37–68
Stephan H, Andy OJ (1969) Quantitative comparative neuroanatomy of primates: an attempt at a phylogenetic interpretation. Ann N Y Acad Sci 167(1):370–387
Symington J (1916) Endocranial casts and brain form: a criticism of some recent speculations. J Anat Physiol 50(Pt 2):111–130
Zollikofer CP (2002) A computational approach to paleoanthropology. Evol Anthropol: Issues News Rev 11(S1):64–67